

## Strengthening poly(2-hydroxyethyl methacrylate) hydrogels using biochars and hydrophobic aggregations

Ping Zhang, Ziyi Xu, Zhiying Wu, Ping Xu & Canhui Yang

To cite this article: Ping Zhang, Ziyi Xu, Zhiying Wu, Ping Xu & Canhui Yang (2022): Strengthening poly(2-hydroxyethyl methacrylate) hydrogels using biochars and hydrophobic aggregations, International Journal of Smart and Nano Materials, DOI: [10.1080/19475411.2022.2107115](https://doi.org/10.1080/19475411.2022.2107115)

To link to this article: <https://doi.org/10.1080/19475411.2022.2107115>



© 2022 The Author(s). Published by Informa UK Limited, trading as Taylor & Francis Group.



Published online: 02 Aug 2022.



[Submit your article to this journal](#)



Article views: 185



[View related articles](#)



[View Crossmark data](#)



# Strengthening poly(2-hydroxyethyl methacrylate) hydrogels using biochars and hydrophobic aggregations

Ping Zhang<sup>a\*</sup>, Ziyi Xu<sup>a\*</sup>, Zhiying Wu<sup>b</sup>, Ping Xu<sup>c</sup> and Canhui Yang<sup>a</sup>

<sup>a</sup>Shenzhen Key Laboratory of Soft Mechanics & Smart Manufacturing, Department of Mechanics and Aerospace Engineering, Southern University of Science and Technology, Shenzhen, P. R. China;

<sup>b</sup>Department of Chemistry, City University of Hong Kong, Hong Kong, P.R. China; <sup>c</sup>Department of Respiratory and Critical Care Medicine, Peking University Shenzhen Hospital, Shenzhen, Guangdong, P. R. China

## ABSTRACT

As the first version of synthetic hydrogel, poly(2-hydroxyethyl methacrylate) hydrogels have found broad applications. However, their poor mechanical performances have been long-standing hurdles for practical deployments. Herein, we report on strengthening the poly(2-hydroxyethyl methacrylate) hydrogels with biochar nanoparticles and hydrophobic aggregations, which are induced by solvent exchange and reinforced by freeze-thaw. Both the vast anchoring points on the multifunctional surfaces of the biochar nanoparticles and the aggregates formed between poly(2-hydroxyethyl methacrylate) chains engender strong and dissipative physical crosslinks. The resulting hydrogels exhibit marked mechanical properties, encompassing high stretchability  $\sim 7$ , high fracture toughness  $\sim 1360 \text{ J m}^{-2}$ , high elastic modulus  $\sim 180 \text{ kPa}$ , low friction coefficient  $\sim 0.2$ , self-recovery, and non-swellability. Furthermore, we demonstrate the versatility of the proposed strategy by using water/ionic liquid binary solvent as the solvent system, Laponite as the nano-reinforcement, and dry-anneal as the hydrophobic aggregation enhancer to synthesize mechanically robust hydrogels. Poly(2-hydroxyethyl methacrylate) hydrogels of superior mechanical properties are expected to enable previously inaccessible applications in biomedicine and engineering.



## ARTICLE HISTORY

Received 10 June 2022

Accepted 25 July 2022

## KEYWORDS

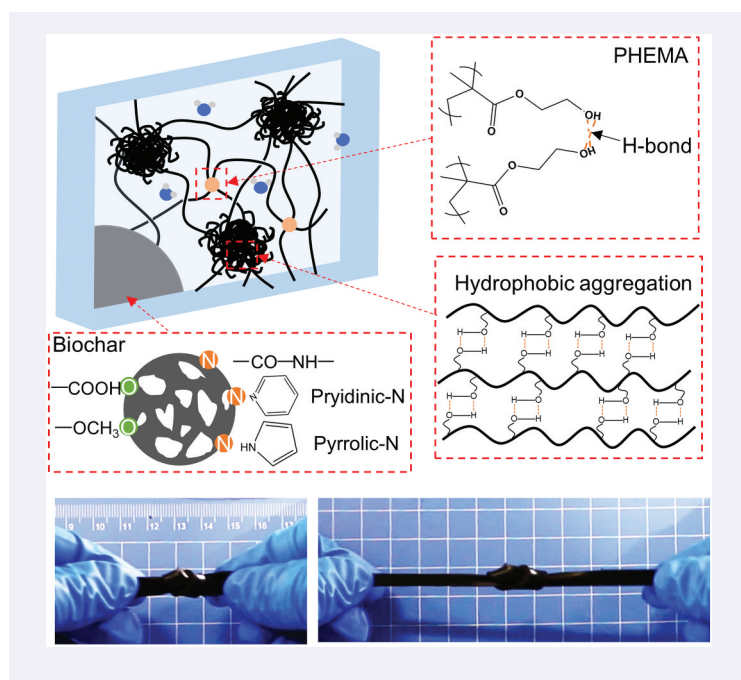
Hydrogel; PHEMA; mechanical properties; biochar; hydrophobic aggregation

**CONTACT** Canhui Yang  [yangch@sustech.edu.cn](mailto:yangch@sustech.edu.cn)  Shenzhen Key Laboratory of Soft Mechanics & Smart Manufacturing, Department of Mechanics and Aerospace Engineering, Southern University of Science and Technology, Shenzhen 518055, P. R. China

\*These authors equally contributed to this work.

© 2022 The Author(s). Published by Informa UK Limited, trading as Taylor & Francis Group.

This is an Open Access article distributed under the terms of the Creative Commons Attribution License (<http://creativecommons.org/licenses/by/4.0/>), which permits unrestricted use, distribution, and reproduction in any medium, provided the original work is properly cited.



## 1. Introduction

As the first version of synthetic hydrogel, poly(2-hydroxyethyl methacrylate) (PHEMA) hydrogel was invented for biological use: soft contact lens [1]. Immediately after the invention, enormous researches have been taking place in exploiting PHEMA hydrogels for a wide range of bio-applications as diverse as tissue regeneration [2,3], tissue replacements [4,5], drug delivery vehicles [6,7], wound dressings [8,9], and nerve guidance channels [10], owing to its outstanding biocompatibility, hydrophilicity, optical transparency, and nontoxic nature [3]. Non-biological utilizations such as actuators [11] and pH and ionic strength sensors [12] have also been explored. However, conventionally crosslinked single network PHEMA hydrogels are weak and brittle, imposing formidable obstacles that bottleneck their deployments and further developments. As such, improving the mechanical properties sensibly becomes one of the prerequisites for the practical applications of PHEMA hydrogels.

The general principle of strengthening a hydrogel is to introduce efficient energy dissipation mechanism into the hydrogel matrix meanwhile maintain the high elasticity of the polymer network [13,14]. Following this principle, various strategies have been proposed over the past decades to make mechanically robust hydrogels, including double-network hydrogels [15–17], nanocomposite hydrogels [18–21], topological hydrogels [22], polyampholyte hydrogels [23], hydrogel composites [24–26], and hydrogels containing crystalline structures [27]. Putting these strengthening methods into effect, PHEMA hydrogels with improved mechanical properties have been synthesized. For example, Sun and coauthors interpenetrate the covalent PHEMA network with a physical alginate network, forming a stiff and tough PHEMA-alginate double network hydrogel [28]. Zhao et. al incorporates carbon nanotubes into the precursor of PHEMA,

deposits the mixture through an extrusion nozzle which exerts the shear-induced alignment, and photo-cures the mixture to obtain a nanocomposite PHEMA hydrogel with anisotropic mechanical and electrical properties [29]. Young et. al introduces various kinds of weaved and knitted fabrics and fibers as the dissipaters into the matrix to obtain tough PHEMA hydrogels [30]. He et al. toughens PHEMA hydrogels by MXenes and uses the resulting MXene/PHEMA hydrogel as a strain sensor for underwater sensing [31]. Despite the encouraging processes, limitations of existing works have been noted: existing methods are often exclusive that it is compulsive to re-design the material systems and re-optimize the synthetic procedure once the constituents of the hydrogel change. Thus, ameliorating the mechanical performances of PHEMA hydrogels remains a challenge.

Herein, we report on a versatile strategy to strengthen the PHEMA hydrogels by synergistically invoking two mechanisms: nano-reinforcements and hydrophobic aggregations. The former provides abundant anchoring points for polymer chains and the latter allows for dense chain aggregates, both of which facilitate the formation of strong and dissipative physical crosslinks. We exemplify the strategy by using the biochar nanoparticles and the aggregates induced by the solvent exchange process as the specific embodiments. As a representative implementation case, we homogeneously mix the biochar nanoparticles with HEMA monomers and initiators in a water/alcohol binary solvent, cure the mixture into a biochar/PHEMA gel, and replace the alcohol with water to trigger the hydrophobic aggregations, which is further enhanced by freeze-thaw cycles. The resulting physically crosslinked biochar/PHEMA nanocomposite hydrogel is stretchable, tough, low friction, self-recovery, and stable against swelling. Moreover, we demonstrate the versatility of the method by altering the synthetic conditions, including using water/ionic liquid binary solvent as the solvent system, Laponite as the nano-reinforcement, and dry-anneal as the hydrophobic aggregation enhancer, and consistently obtain strong hydrogels. This work offers an alternative yet efficient and general means toward HEMA hydrogels of excellent mechanical properties.

## 2. Results and discussions

As shown in Figure 1a, we start by polymerizing HEMA monomers in a water/alcohol binary solvent system without adding any covalent crosslinkers. The resulting PHEMA hydrogel contains 56% solvent and a network of long PHEMA chains physically crosslinked by the hydrogen bonds between the pendant groups of adjacent PHEMA chains, e.g. hydroxyl groups. Compared to the covalently crosslinked PHEMA network, the physically crosslinked PHEMA network has longer polymer chains which are beneficial for energy dissipation, especially under fatigue circumstances [32], and has the merits of being self-recovery and/or even self-healing. We then conduct solvent exchange by immersing the PHEMA hydrogel into deionized water, during which the alcohol molecules are replaced by water molecules. Since the PHEMA polymer chain involves hydrophobic segments originating from methyl derivatives [33], the saturated water content of PHEMA hydrogel is about 40 wt%, such that solvent exchange causes the PHEMA hydrogel to undergo hydrophobic aggregations, which has been manipulated to regulate noncovalent interchain interactions for mechanically strong hydrogels [34,35]. The hydrophobic aggregates allow for the formation of more interchain hydrogen bonds meanwhile expel a certain amount of water. The PHEMA hydrogel at this stage has a lower solvent content, i.e. water, of about

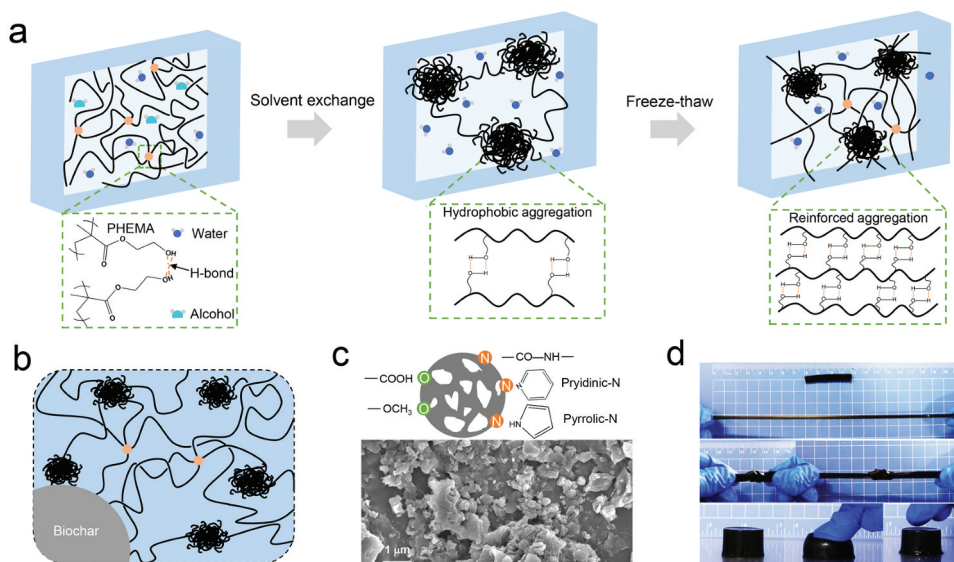


**Figure 1.** Schematic of the strengthening mechanism. (a) A homogeneous physically crosslinked PHEMA hydrogel is first synthesized with a water/alcohol binary solvent. The alcohol is replaced by water via a solvent exchange process to trigger the hydrophobic aggregations between PHEMA chains. The aggregation is further reinforced by freeze-thaw, resulting. (b) Biochar nanoparticles are incorporated into the hydrogel matrix, providing abundant anchoring sites for PHEMA chains. (c) The chemical structure and the SEM image of biochar nanoparticles. (d) Photos illustrating the mechanical robustness of 2-biochar/PHEMA hydrogel: stretching, knotting and stretching, and compression.

50 wt%. Subsequently, we perform the freeze-thaw cycles for the hydrogel, which further reinforces the hydrophobic aggregations by densifying the interchain hydrogen bonds. The reinforced aggregates accommodate hidden polymer chains that can simultaneously promote the stiffness, the strength, and the fracture toughness of hydrogels [36].

In addition to the hydrophobic aggregation, we further bolster the mechanical strength of the PHEMA hydrogel by incorporating biochar nanoparticles into the hydrogel matrix (Figure 1b). Biochar, normally obtained through the thermal decomposition of biomass under oxygen-limited conditions, features highly-porous structures, large surface areas, and various oxygen functional groups and thus provides abundant anchoring sites for the PHEMA chains. Figure 1c schematizes the possible chemical structure [37] and shows the microscopic photography of the biochar nanoparticles, implying an average size of about 300 nm. Upon loading, the anchored PHEMA chains will be stretched tight and then detached from the surfaces of the biochar nanoparticles, releasing all of the strain energy once stored over the entire PHEMA chains. Such molecular-scale energy dissipater mechanism also applies to the hydrophobic aggregations and reaffirms the significance of a covalent crosslinks-free PHEMA network of long polymer chains. Leaving the detail optimizations for later, we demonstrate the exceptional mechanical properties of as-prepared 2-biochar/PHEMA (the terminology will be explained in the next section) hydrogel by stretching and knotting and stretching a hydrogel stripe to about 5 times its original length, and violently compressing a hydrogel cylinder which can spring back without noticeable damage after unloading (Figure 1d).

Crucial for our strengthening method is the use of a binary solvent system, the solvent exchange process, the freeze-thaw process, and the inclusion of biochar nanoparticles. We carry out a stepwise comparison between different hydrogels by invoking the pure shear test and comparing their fracture toughness. The pure shear test was first proposed by Rivlin and Thomas to characterize the toughness of rubber [38], and has been widely adopted ever since for other soft and stretchable materials including hydrogels [16]. Geometrically, the test indicates that the sample has a length (perpendicular to the loading direction) much larger than the width (along the loading direction), which in turn is much larger than the thickness. In our experiments, the samples are 70 mm in length, 10 mm in width, and 2 mm in thickness. Figure 2a collects the nominal stress-strain curves of different hydrogels. Here 1-PHEMA-water represents the hydrogel synthesized in deionized water, 1-PHEMA represents the hydrogel synthesized in water/alcohol binary solvent system, 2-PHEMA represents the 1-PHEMA hydrogel after solvent exchange, 1-biochar/PHEMA represents the biochar/PHEMA hydrogel synthesized in water/alcohol binary solvent system, 2-biochar/PHEMA represents the 1-biochar/PHEMA hydrogel after solvent exchange, and 3-biochar/PHEMA represents the 2-biochar/PHEMA hydrogel after freeze-thaw. It can be seen that the hydrophobic aggregations significantly enhance the strength of the

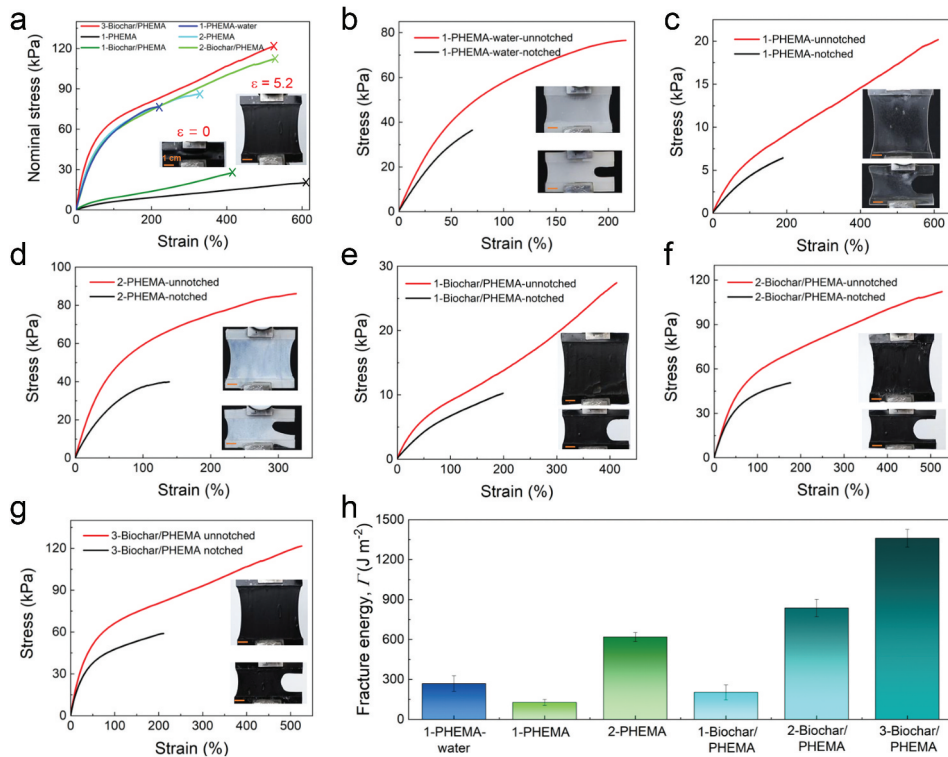


**Figure 2.** Fracture properties of various PHEMA hydrogels under pure shear test. (a) The nominal stress-strain curves of various hydrogels. The insets show the undeformed and deformed states of the 3-biochar/PHEMA hydrogel. The stress-strain curves of unnotched and notched samples of (b) 1-PHEMA-water, (c) 1-PHEMA, (d) 2-PHEMA, (e) 1-biochar/PHEMA, (f) 2-biochar/PHEMA, and (g) 3-biochar/PHEMA hydrogels. (h) The fracture energies of various hydrogels.



hydrogel (light blue curve vs black curve, light green curve vs dark green curve). Although the endowment of biochar nanoparticles alone does not exhibit noteworthy enhancement, the synergy between biochar nanoparticles and the hydrophobic aggregations profoundly increases the mechanical performances (light green curve vs black curve). Note that whereas the strength of the 1-PHEMA-water is higher than that of the 1-PHEMA hydrogel, its stretchability is much limited. The 3-biochar/PHEMA hydrogel, as expected, exhibits the best mechanical properties, signifying the role of the reinforced hydrophobic aggregation. The insets show the 3-biochar/PHEMA hydrogel at  $\varepsilon = 0$  and  $\varepsilon = 5.2$ .

To measure the fracture toughness, two sets of samples of identical dimensions are required, with one being precut with a single-edge notch along the middle line of the sample and the other being intact. For the notched samples, we make a pre-crack of 20 mm using a razor blade. The size of the pre-crack is much larger than the width while much smaller than the length of the sample. The nominal stress-strain curves of various unnotched/notched hydrogels are plotted in Figures 2(b–g), respectively, along with their corresponding deformation states at the verge of fracture shown in the insets. The unnotched samples are stretched (may or may not up to rupture) and their stress-strain curves are measured, denoted as red curves. The notched samples are stretched until the notch started to propagate catastrophically at a critical strain  $\varepsilon_c$ , and their stress-strain curves are denoted in black. Fracture toughness of the hydrogel is calculated by  $\Gamma = H \cdot W(\varepsilon_c)$ , where  $H$  is the effective width at the undeformed state and  $W(\varepsilon_c)$  is the strain energy density of the unnotched sample, calculated as the integration of the stress-strain curve up to  $\varepsilon_c$ .

$$W(\varepsilon_c) = \int_0^{\varepsilon_c} \sigma(\varepsilon) d\varepsilon.$$
 Figure 2(h) shows the histogram of the average toughness of different hydrogels, with  $269.0 \text{ J m}^{-2}$  for 1-PHEMA-water,  $127.6 \text{ J m}^{-2}$  for 1-PHEMA,  $618.9 \text{ J m}^{-2}$  for 2-PHEMA,  $203.3 \text{ J m}^{-2}$  for 1-biochar/PHEMA,  $836.5 \text{ J m}^{-2}$  for 2-biochar/PHEMA, and  $1367.7 \text{ J m}^{-2}$  for 3-biochar/PHEMA hydrogels, respectively.

Now that we have manifested the highest fracture toughness of the 3-biochar/PHEMA hydrogel, we next systematically characterize its performances. SEM images show that the biochar nanoparticles are well dispersed within the hydrogel despite of somewhat conglomeration (bottom-right magnified inset) and the clusters due to the hydrophobic aggregations of PHEMA chains (top-right magnified inset) (Figure 3a). Figure 3b shows the uniaxial nominal stress-strain curves measured using dumbbell-shaped specimens, giving a fracture strain exceeding 600%. To examine the energy dissipating capacity of the hydrogel, we perform cyclic load and unload test with varying maximum strains before unloading. Figure 3c plots the stress-strain curves of maximum strain varying from 1 to 6, and pronounced loop enclosed between the loading and unloading curves persists for all maximum strains, indicative of a dissipative matrix. The area of the loop denotes the energy dissipation during that load and unload cycle,  $W_D$ . Dividing  $W_D$  by the area underneath the loading curve, i.e. the work done by external forces, yields the hysteresis. Notably, the hysteresis of the 3-biochar/PHEMA hydrogel is larger than 60% regardless of the maximum strain, and the highest hysteresis of ~80% is achieved at the maximum strain  $\varepsilon = 4$  (Figure 3d). We understand this tendency as follows. Keep in mind that the work done by external work is converted into two types of energy: the dissipated energy and the elastic strain energy stored in the polymer network. The energy dissipation might stem from the breaking of hydrogen bonds between PHEMA chains, the detachments of

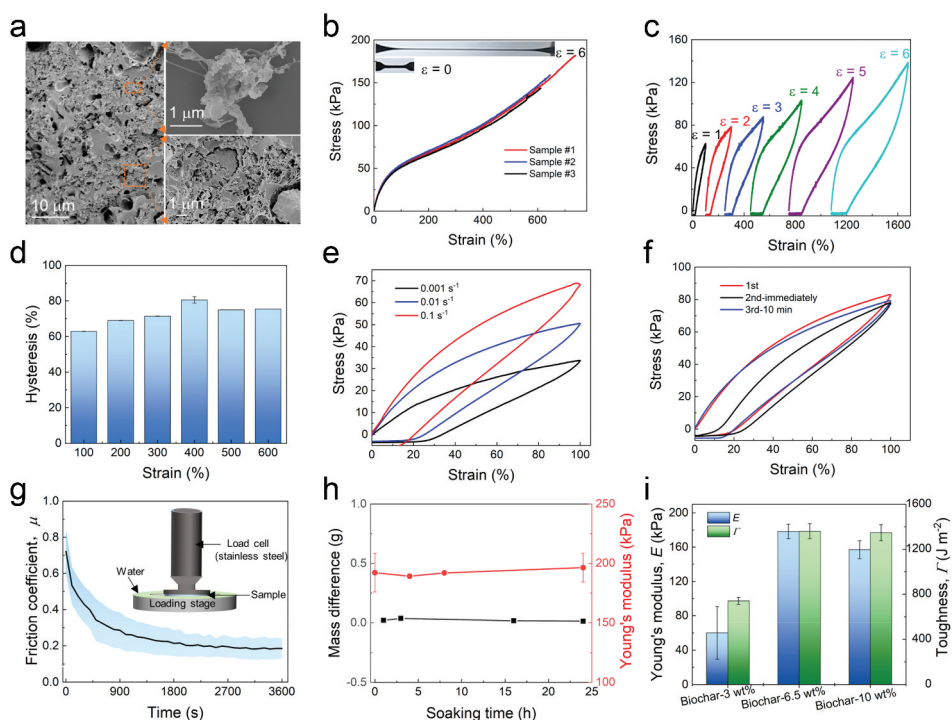


**Figure 3.** Characterizations of 3-biochar/PHEMA hydrogel. (a) SEM photographs of the freeze-drying sample. (b) Uniaxial tensile stress-strain curves. (c) Cyclic load-unload curves with different maximum strains before unloading. (d) Hysteresis varies with strain. (e) Cyclic load-unload curves with different strain rates. (f) Recovery test. (g) Friction test. (h) The variations of mass and Young's modulus with the soaking time. (i) Young's modulus  $E$  and toughness  $\Gamma$  vary with the content of biochar nanoparticles.

PHEMA chains from the surfaces of biochar nanoparticles, as well as the interchain friction due to chain disentanglements and pull-out. Whereas the interchain friction, in principle, can occur under any deformation, the breaking of hydrogen bonds between PHEMA chains and the detachments of PHEMA chains from the surfaces of biochar particles require certain stress (i.e. certain deformation). Consequently, as the deformation increases, the dissipated energy due to bond-breaking becomes more and more pronounced and the hysteresis increases. However, as the deformation becomes too large, the rate of the increase of dissipated energy plateaus or even decreases, meanwhile, the elastic energy catches up as the strain-hardening state is approached. Overall, the maximum hysteresis is obtained at an intermediate strain.

Recall that the 3-biochar/PHEMA hydrogel is physically crosslinked by biochar nanoparticles and hydrogen bonds. These physical interactions, on one hand, make the hydrogel matrix viscoelastic that the hysteresis decreases from 79% to 55% when the strain rate varies from  $0.001 \text{ s}^{-1}$  to  $0.1 \text{ s}^{-1}$  (Figure 3e). Rather, both the Young's modulus and the peak stress increase with the strain rate, the characteristics of viscoelastic materials. On the other hand, the regeneration of the physical interactions after break facilitates the self-recovery. For instance, the 3-biochar/PHEMA hydrogel already regains 78.6% of hysteresis in the second cycle of a consecutive load and unload with a maximum strain of 100%, and recovers by 98.9% in the third cycle after 10 minutes of rest (Figure 3f).



The recovery is likely ascribed to the re-anchoring of PHEMA chains on the surfaces of biochar nanoparticles and the reversible entanglement/disentanglement of the hydrophobic associations within the aggregations [39]. The prominent viscoelasticity of the 3-biochar/PHEMA hydrogel should be ascribed to the noncovalent interactions within the hydrogel matrix, including the hydrogen bonds between PHEMA chains and the physical anchoring of PHEMA chains on the biochar nanoparticles. We have simply investigated the viscoelasticity by stretching the hydrogels using different velocities, but the noncovalent interactions can lead to much more sophisticated behaviors, for example, influencing the dynamic moduli at both high and low frequencies in dynamic deformation [40,41]. However, further pursuing the details of the noncovalent interactions is beyond the scope of current work.

In many biological scenarios such as the cartilage replacement and the contact lens, the friction of hydrogels is pivotal for the sake of minimal abrasion. We characterize the lubricating performances of the 3-biochar/PHEMA hydrogel by measuring its friction coefficient. As schematized in the inset of Figure 3g, we apply an axial force on the sample and measure the torque needed to rotate the load cell at  $1 \text{ rad s}^{-1}$  using a rheometer [42]. The friction coefficient  $\mu$ , which is calculated by  $\mu = 4 T/3RF$ , where  $T$  is the torque,  $R$  is the diameter of the load cell, and  $F$  is the normal force, is plotted against time. The friction coefficient gradually decreases with time and stabilizes at about 0.2 after 2000 seconds. Another commonly overlooked issue of hydrogels is swelling. Conventional hydrogels tend to swell in water and become soft and fragile, detrimentally limiting their practical applicability in a water-rich physiological environment. Surprisingly, the 3-biochar/PHEMA hydrogel turns out to be stable against swelling that its mass and Young's modulus barely change after being soaked in deionized water for 24 hours (Figure 3h). Such non-swellability is possibly thanks to the limited solubility between PHEMA chains and water as well as the strong crosslinks of the PHEMA network. So far, the content of biochar nanoparticles in the 3-biochar/PHEMA hydrogel has been taken for granted. We investigate the effects of biochar on the mechanical properties of hydrogels and obtain an optimized content of 6.5 wt%, which renders Young's modulus of 178.3 kPa and fracture toughness of  $1367.7 \text{ J m}^{-2}$ , respectively (Figure 3i).

Our strengthening strategy relies on the synergy of nano-reinforcements and hydrophobic aggregations. Whereas we have specifically selected the 3-biochar/PHEMA hydrogel for illustration, the strengthening principle generally applies to other material systems. Without losing generality, we will stay with PHEMA hydrogels and demonstrate the versatility of the strengthening strategy. First, we replace the alcohol in the binary solvent system with an equal mass of ionic liquid, 1-butyl-3-methylimidazolium chloride ([Bmim] Cl), whose chemical structure is delineated in Figure 4a. The resulting hydrogel is termed as 3-biochar/PHEMA@[Bmim]Cl, which can be uniaxially stretched to a strain of  $\sim 5$  (Figure 4b) and possesses fracture toughness of  $1530 \text{ J m}^{-2}$ . Second, we use another commonly used inorganic nanoclay, lithium magnesium silicate, also known as Laponite, as the nano-reinforcer to synthesize the hydrogel (Figure 4d). Laponite is made up of 2-dimensional disk-shaped nanosheets that are decorated with myriad negative charges and act as the multifunctional crosslinking spots for the berthing of polymer chains through ionic or polar interactions [43]. Again, the resulting 3-Laponite/PHEMA hydrogels are stretchable and tough, exhibiting a fracture strain of  $\sim 4$  (Figure 4e) and fracture toughness of  $1460 \text{ J m}^{-2}$  (Figure 4f). Last but not least, we modify the hydrophobic aggregation enhancing method

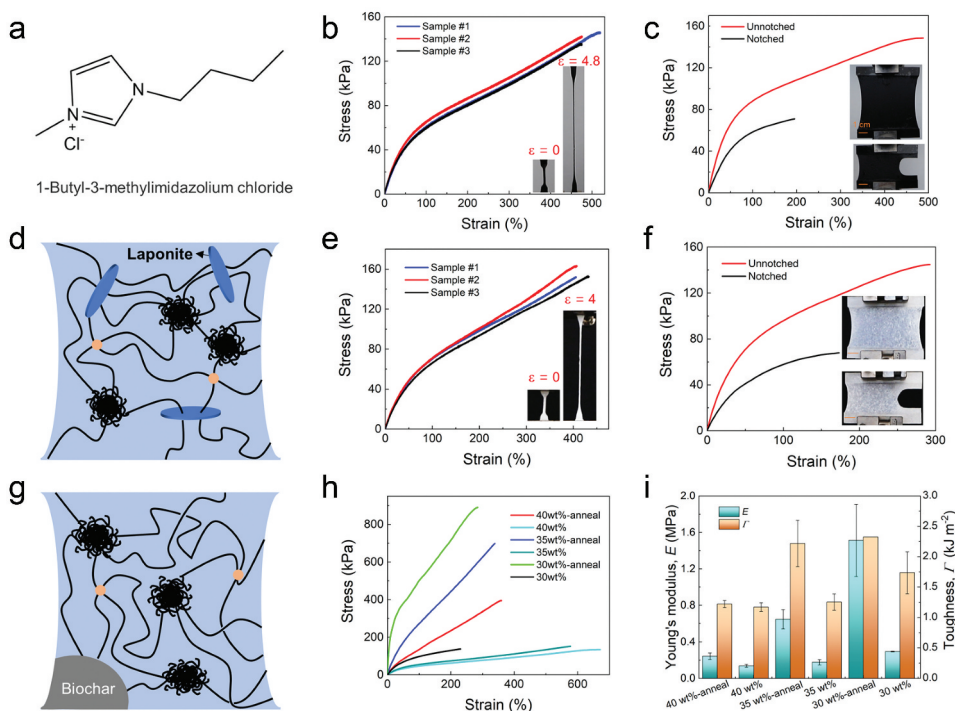


**Figure 4.** Versatility of the strengthening strategy. (a) The chemical structure of 1-butyl-3-methylimidazolium chloride for water/ionic liquid binary solvent. (b) Uniaxial tensile test of 3-biochar/PHEMA@[Bmim]Cl. The insets are the snapshots during tension. (c) Fracture toughness measured by pure shear test. (d) Schematic of nanocomposite hydrogel with Laponite as the reinforcement. Uniaxial tensile test (e) and pure shear test (f) of 3-Laponite/PHEMA hydrogel. (g) Schematic of 3-biochar/PHEMA hydrogel after dry-anneal. (h) Uniaxial tensile stress-strain curves and (i) Young's modulus and toughness of biochar/PHEMA hydrogels of different water contents and with/without annealing as indicated.

by using the dry-anneal treatment, wherein the drying process is performed at room temperature and the annealing process is performed at 105°C. After the dry-anneal treatment, the samples are immersed in deionized water to obtain the 3-biochar/PHEMA hydrogel, in which the hydrophobic aggregates are denser and the crosslinks of hydrogen bonds are stronger (Figure 4g). We control the swelling degree of the samples and use  $x$  wt %-anneal to denote the hydrogels experiencing anneal and containing  $x$  wt% water. It should be pointed out that the water content at swelling equilibrium is about 40 wt% for the annealed hydrogels while the equilibrium water content of the hydrogel after solvent exchange can reach 50 wt%, another clue for the enhanced hydrophobic aggregation. We swell the annealed samples to 30 wt%, 35 wt%, and 40 wt% water content and deswell the hydrogels after solvent exchange to the same water contents for comparison. The uniaxial tensile stress-strain curves of the six types of hydrogels are plotted in Figure 4h. All hydrogels become stiffer and less stretchable as the water content decreases. For the same water content, the hydrogels with annealing are much stiffer and stronger than those without annealing (Figure 4i). Also, the fracture toughness of annealed hydrogel is higher than that of unannealed hydrogel. In addition, in the stability against swelling in water, the

mass change of the annealed 3-biochar/PHEMA hydrogel (containing 40 wt% water) is nearly zero, whereas the 2-biochar/PHEMA hydrogel (containing 40 wt% water as well) swells and gains 10 wt% extra mass.

### 3. Conclusion

In conclusion, we report a general strengthening strategy for mechanically robust PHEMA hydrogels by synergistically invoking the nano-reinforcements and the hydrophobic aggregations mechanisms. Using biochar nanoparticles and solvent exchange, we achieve biochar/PHEMA hydrogels of high stretchability, high toughness, high modulus, low friction coefficient, self-recovery, and non-swellability. Additionally, we demonstrate the universality of the proposed method with three different amendments to the synthetic procedure, all of which lead to strong PHEMA hydrogels. Because PHEMA hydrogels are among the most investigated biomaterials, it is envisioned that current work will help pave new avenues to make PHEMA hydrogels, as well as hydrogels of other chemistries that can form aggregates or even crystalline structures such as chitosan and polyvinyl alcohol. Hydrogels with extraordinary mechanical properties provide potential solutions to meet the challenges exerted by a wide range of applications, such as tissue replacements [5], drug delivery [6], wound dressings [8], water treatment [18], as well as sensors and actuators for soft robotics [11,12].

### 4. Experimental section

#### *Materials*

We purchased N, N, N', N' – tetramethylethylenediamine (TEMED, T105497) and 2-hydroxyethyl methacrylate (HEMA, H103044) from Aladdin, sodium persulfate (APS, S817729) from Mackling, ethanol (B2109131) from Xilong Scientific Co. Ltd, lithium magnesium silicate (Laponite, S24861) from Shanghai Yuanye Bio-Technology Co. Ltd, and 1-butyl-3-methylimidazolium chloride ([Bmim]Cl, K101090) from Shanghai Deepak Biotechnology Co. Ltd. All chemicals were used without further purification.

#### *Synthesis of 1-PHEMA-water, 1-PHEMA, and 2-PHEMA*

First, 5.94 g APS was completely dissolved in 85.13 g deionized water at 40°C. Then, 52.65 g HEMA and 108  $\mu$ L TEMED were added and stirred to form a homogeneous mixture. The mixture was poured into a glass mold (200 mm  $\times$  200 mm  $\times$  2 mm), which was coated with release films on the surfaces for easy demolding, and cured in a 40°C oven for 24 hours. The resulting 1-PHEMA-water hydrogel contains 56 wt% water and appears to be opaque due to phase separation.

Likewise, 5.94 g APS was dissolved in a mixed solution composed of 56.00 g deionized water and 45.00 g ethanol at 40°C, followed by adding 52.65 g HEMA and 108  $\mu$ L TEMED. After curing at 40°C for 24 hours, a transparent 1-PHEMA gel containing 56 wt% solvent is obtained. The 1-PHEMA gel was further soaked into pure water for 24 hours, during which the alcohol molecules were substituted by water molecules, resulting in the 2-PHEMA hydrogel containing 50 wt% water.

### ***Synthesis of 1-biochar/PHEMA, 2-biochar/PHEMA, and 3-biochar/PHEMA***

First, biochar and deionized water were mixed at a certain weight ratio in a mill pot and ball-milled for 120 minutes at a speed of 300 rpm to transform the solid-liquid amalgam into a homogeneous biochar slurry. Then 5.94 g APS, 52.65 g HEMA, and 108  $\mu\text{L}$  TEMED were sequentially added into the solution of the biochar slurry (67.2 g) and ethanol (45 g). After being poured into a glass mold and cured, the 1-biochar/PHEMA hydrogel of 59 wt% solvent was obtained.

The 1-biochar/PHEMA hydrogel was soaked into deionized water for 24 hours to obtain the 2-biochar/PHEMA hydrogel of 50 wt% water. The 2-biochar/PHEMA hydrogel was further frozen at  $-18^{\circ}\text{C}$  for about 8 hours and thawed at  $25^{\circ}\text{C}$  for 3 hours. The freeze-thaw process is repeated 7 times to form the 3-biochar/PHEMA hydrogel of 40 wt% water content.

### ***Synthesis of biochar/PHEMA@[Bmim]Cl hydrogel, Laponite/PHEMA hydrogel, and dry-annealed biochar/PHEMA hydrogel***

The synthetic procedure of biochar/PHEMA@[Bmim]Cl hydrogel is identical to that of the 3-biochar/PHEMA hydrogel except that the alcohol was replaced by [Bmim]Cl of the same mass. The synthetic procedure of Laponite/PHEMA hydrogel is identical to that of the 3-biochar/PHEMA hydrogel except that 2.8 g Laponite instead of biochar nanoparticles was used for the nano-reinforcers. For the dry-anneal biochar/PHEMA hydrogel, the freeze-thaw cycles were replaced by the dry-anneal procedure, which included desiccating 2-biochar/PHEMA hydrogel at room temperature for 5 hours, annealing the hydrogel at  $105^{\circ}\text{C}$  for 2 hours, and then re-swelling the hydrogel in water with controlled water contents.

### ***Mechanical characterizations***

For tensile tests, the samples were cut into a dumbbell shape (gauge length 15 mm, width 2 mm, thickness 2 mm). Both ends of the samples were clamped, loaded on a mechanical testing machine (Instron 5966), and stretched at a loading velocity of  $30\text{ mm min}^{-1}$  with a 100 N load cell. The nominal tensile stress was calculated as  $\sigma = F/A_0$ , where  $F$  is the magnitude of the load and  $A_0$  is the original cross-sectional area of the sample. The nominal tensile strain ( $\epsilon$ ) was calculated as  $\epsilon = \Delta l/l_0 \times 100\%$ , where  $\Delta l$  is the change of gauge length relative to its initial length ( $l_0$ ). A digital camera was used to record the elongation process, which was proceeded for calibration of the deformation of the gauge length.

For the pure shear test, two sets of samples of length 70 mm, width 30 mm, and thickness 2 mm were prepared. One had no notch and the other was pre-notched to form a 20 mm-long single-edge notch using a razor. After being loaded to the testing machine, the effective width (along the loading direction) of the sample is 10 mm. The samples are pulled and their stress-strain curves are measured.

The friction coefficients were measured in water at  $25^{\circ}\text{C}$  using a rheometer (HR-30, TA Instruments). All samples were cut into a disk shape with a dimension of  $20\text{ mm} \times 20\text{ mm} \times 2\text{ mm}$  and glued to the loading stage of the rheometer. The load cell (parallel plate,

20 mm in diameter) was applied on the surface of the sample with a normal force of 5 N. The torque and the normal force were recorded when the load cell rotated at an angular velocity of  $1 \text{ rad s}^{-1}$ .

### Materials characterizations

The morphology and microstructure of the ball-milled biochar and freeze-dried hydrogels were examined using a high-resolution scanning electron microscope at the operating voltage of 3–5 kV (Hitachi, SU8200, Japan).

The swelling behaviors were probed by soaking the samples of 2-biochar/PHEMA hydrogels, 3-biochar/PHEMA hydrogels, and dry-anneal biochar/PHEMA hydrogels into deionized water. The mass of each sample was measured at 0 hours, 1 hour, 3 hours, 16 hours, and 24 hours.

### Acknowledgments

P. X. acknowledges the support from Shenzhen Science and Technology Innovation Commission Foundation (No.20206238).

### Disclosure statement

No potential conflict of interest was reported by the author(s).

### Funding

The work at the Southern University of Science and Technology is supported by the Natural Science Foundation of Guangdong Province [2214050008118], the Stable Support Plan Program of Shenzhen Natural Science Fund Grant [K21326303], and the Science, Technology, and Innovation Commission of Shenzhen Municipality [ZDSYS20210623092005017].

### References

- [1] Wichterle O, Lim D. Hydrophilic gels for biological use. *Nature*. 1960;185(4706):117–118.
- [2] Zhao F, Yao D, Guo R, et al. Composites of polymer hydrogels and nanoparticulate systems for biomedical and pharmaceutical applications. *Nanomaterials (Basel)*. 2015;5:2054–2130.
- [3] Zare M, Bigham A, Zare M, et al. PHEMA: an overview for biomedical applications. *Int J Mol Sci*. 2021;22(12):6376.
- [4] Chen L, Tang Y, and Zhao K, et al. HEMA-Modified Expandable P(MMA-AA) Bone Cement with Dual Water Absorption Networks. *Macromol Mater Eng*. 2020; 305.
- [5] Janáček J. *Journal of macromolecular science, part C. Polymer Rev*. 1973;9:3–47.
- [6] Filippousi M, Siafaka PI, Amanatiadou EP, et al. Modified chitosan coated mesoporous strontium hydroxyapatite nanorods as drug carriers. *J Mater Chem B*. 2015;3(29):5991–6000.
- [7] Ribeiro A, Veiga F, Santos D, et al. Bioinspired imprinted PHEMA-Hydrogels for ocular delivery of carbonic anhydrase inhibitor drugs. *Biomacromolecules*. 2011;12(3):701–709.
- [8] Jacob S, Nair AB, Shah J, et al. Optimisation of the Chicken Chorioallantoic Membrane Assay in Uveal Melanoma Research. *Pharmaceutics*. 2021;14:13.
- [9] Di Z, Shi Z, Ullah MW, et al. A transparent wound dressing based on bacterial cellulose whisker and poly(2-hydroxyethyl methacrylate). *Int J Biol Macromol*. 2017;105:638–644.

- [10] Dalton PD, Flynn L, Shoichet MS. Manufacture of poly(2-hydroxyethyl methacrylate-co-methyl methacrylate) hydrogel tubes for use as nerve guidance channels. *Biomaterials*. [2002](#);23(18):3843–3851.
- [11] Li J, Chee HL, and Chong YT , et al. Hofmeister Effect Mediated Strong PHEMA-Gelatin Hydrogel Actuator. *ACS Appl Mater Interfaces*. [2022](#); 14: 23826–23838.
- [12] Jia X, Wang K, Wang J, et al. Full-color photonic hydrogels for pH and ionic strength sensing. *Eur Polym J*. [2016](#);83:60–66.
- [13] Zhao X. Multi-scale multi-mechanism design of tough hydrogels: building dissipation into stretchy networks. *Soft Matter*. [2014](#);10(5):672–687.
- [14] Yang C, Suo Z. Hydrogel ionotronics. *Nat Rev Mater*. [2018](#);3(6):125.
- [15] Gong JP, Katsuyama Y, Kurokawa T, et al. Double-network hydrogels with extremely high mechanical strength. *Adv Mater*. [2003](#);15(14):1155–1158.
- [16] Sun JY, Zhao X, Illeperuma WR, et al. Highly stretchable and tough hydrogels. *Nature*. [2012](#);489:133–136.
- [17] Yang CH, Wang MX, Haider H, et al. Strengthening alginate/polyacrylamide hydrogels using various multivalent cations. *ACS Appl Mater Interfaces*. [2013](#);5(21):10418–10422.
- [18] Wu Z, Zhang P, Zhang H, et al. Tough porous nanocomposite hydrogel for water treatment. *J Hazard Mater*. [2022](#);421:126754.
- [19] Peak CW, Wilker JJ, Schmidt G. A review on tough and sticky hydrogels. *Colloid Polym Sci*. [2013](#);291(9):2031–2047.
- [20] Liu R, Liang S, Tang X-Z, et al. Tough and highly stretchable graphene oxide/polyacrylamide nanocomposite hydrogels. *J Mater Chem*. [2012](#);22(28):14160–14167.
- [21] Huang Y, Xiao L, Zhou J, et al. Mechanical enhancement of graphene oxide-filled chitosan-based composite hydrogels by multiple mechanisms. *J Mater Sci*. [2020](#);55(29):14690–14701.
- [22] Liu C, Morimoto N, Jiang L, et al. Tough hydrogels with rapid self-reinforcement. *Science*. [2021](#);372(6546):1078–1081.
- [23] Sun TL, Kurokawa T, Kuroda S, et al. Physical hydrogels composed of polyampholytes demonstrate high toughness and viscoelasticity. *Nat Mater*. [2013](#);12(10):932–937.
- [24] Tonsomboon K, Butcher AL, Oyen ML. Strong and tough nanofibrous hydrogel composites based on biomimetic principles. *Mater Sci Eng C*. [2017](#);72:220–227.
- [25] Wang Z, Xiang C, and Yao X, et al., *Proceedings of the National Academy of Sciences*, [2019](#), 116, 5967–5972.
- [26] Takahashi R, Sun TL, Saruwatari Y, et al. Creating stiff, tough, and functional hydrogel composites with low-melting-point alloys. *Adv Mater*. [2018](#);30(16):1706885.
- [27] Hua M, Wu S, Ma Y, et al. Strong tough hydrogels via the synergy of freeze-casting and salting out. *Nature*. [2021](#);590(7847):594–599.
- [28] Kim YW, Kim JE, Jung Y, et al. Non-swellable, cytocompatible pHEMA-alginate hydrogels with high stiffness and toughness. *Mater Sci Eng C Mater Biol Appl*. [2019](#);95:86–94.
- [29] Zhao W, Chen L, Hu S, et al. Printed hydrogel nanocomposites: fine-tuning nanostructure for anisotropic mechanical and conductive properties. *Adv Compos Hybrid Mater*. [2020](#);3(3):315–324.
- [30] Young C-D, Wu J-R, Tsou T-L. High-strength, ultra-thin and fiber-reinforced pHEMA artificial skin. *Biomaterials*. [1998](#);19(19):1745–1752.
- [31] He S, Sun X, and Qin Z , et al. Non-Swelling and Anti-Fouling MXene Nanocomposite Hydrogels for Underwater Strain Sensing. *Adv Mater Technol*. [2021](#); 7: 2101343.
- [32] Lake G, and Thomas A, *Proceedings of the Royal Society of London. Series A. Mathematical and Physical Sciences*, [1967](#), 300, 108–119.
- [33] Refojo MF. *J Polymer Sci Part A-1*. [1967](#);5:3103–3113.
- [34] Xu L, Gao S, Guo Q, et al. A solvent-exchange strategy to regulate noncovalent interactions for strong and anti-swelling hydrogels. *Adv Mater*. [2020](#);32(52):2004579.
- [35] Wu M, Chen X, Xu J, et al. Freeze-thaw and solvent-exchange strategy to generate physically cross-linked organogels and hydrogels of curdlan with tunable mechanical properties. *Carbohydr Polym*. [2022](#);278:119003.



- [36] Zhao X, *Proceedings of the National Academy of Sciences*, **2017**, 114, 8138–8140.
- [37] Suo F, You X, Yin S, et al. Preparation and characterization of biochar derived from co-pyrolysis of enteromorpha prolifera and corn straw and its potential as a soil amendment. *SciTotal Environ.* **2021**;798:149167.
- [38] Rivlin R, Thomas AG. Rupture of rubber. I. Characteristic energy for tearing. *J Polym Sci.* **1953**;10(3):291–318.
- [39] Tuncaboylu DC, Sari M, Oppermann W, et al. Tough and self-healing hydrogels formed via hydrophobic interactions. *Macromolecules.* **2011**;44(12):4997–5005.
- [40] Giubertoni G, Burla F, Bakker HJ, et al. Connecting the stimuli-responsive rheology of biopolymer hydrogels to underlying hydrogen-bonding interactions. *Macromolecules.* **2020**;53(23):10503–10513.
- [41] Du C, Zhang XN, Sun TL, et al. Hydrogen-bond association-mediated dynamics and viscoelastic properties of tough supramolecular hydrogels. *Macromolecules.* **2021**;54(9):4313–4325.
- [42] Gong JP, Kagata G, Osada Y. Friction of gels. 4. friction on charged Gels. *The Journal of Physical Chemistry B.* **1999**;103(29):6007–6014.
- [43] Schexnailder P, Schmidt G. Nanocomposite polymer hydrogels. *Colloid Polym Sci.* **2009**;287(1):1–11.